Near Surface Geophysics, 2014, **12**, xxx-xxx doi:10.3997/1873-0604.2014003

Integrating MRS data with hydrologic model - Carrizal Catchment (Spain)

G. Baroncini-Turricchia[1,2,*], A.P. Francés[1], M.W. Lubczynski[1], J. Martínez-Fernández[2] and J. Roy[3]

[1] *ITC-Twente University, Hengelosestraat 99, Enschede, The Netherlands*
[2] *CIALE-Universidad de Salamanca, Calle Duero 12 37185 Villamayor, Salamanca, Spain*
[3] *IGP, cp 48671 csp van Horne, Outremont, QC, Canada H2V 4T9, former ITC*

Received February 2013, revision accepted January 2014

ABSTRACT

Magnetic resonance sounding (MRS) provides quantitative hydrogeological information on hydrostratigraphy and hydraulic parameters of subsurface (e.g. flow and storage property of aquifers) that can be integrated in distributed hydrologic models. The hydraulic parameters are typically obtained by pumping tests. In this study, we propose an MRS integration method based on optimizing MRS estimates of aquifer hydraulic parameters through hydrologic model calibration.

The proposed MRS integration method was applied in the 73 km^2 Carrizal Catchment in Spain, characterized by a shallow unconfined aquifer with an unknown aquifer bottom. 12 MRS survey results were inverted with Samovar 11.3, schematized and integrated in the transient, distributed, coupled, hydrologic, MARMITES-MODFLOW model. As the aquifer bottom was unknown, the aquifer was schematized into one unconfined layer of uniform thickness. For that layer, MRS estimators of specific yield and transmissivity/hydraulic conductivity were calculated as weighted averages of the inverted MRS layers. The MRS integration with hydrologic model was carried out by introducing multipliers of specific yield and transmissivity/hydraulic conductivity that were optimized during transient model calibration using 11 time-series piezometric observation points. The optimized multipliers were 1.0 for specific yield and $3.5*10^{-9}$ for hydraulic conductivity. These multipliers were used, and can be used in future MRS investigations in the Carrizal Catchment (and/or adjacent area with similar hydrogeological conditions), to convert MRS survey results into aquifer hydraulic parameters.

The proposed method of MRS data integration in the hydrologic model of Carrizal Catchment not only allowed us to calibrate the model but also to confirm the functional capability of MRS in quantitative groundwater assessment. Most importantly however, it demonstrated that if pumping tests are not available, the use of MRS integrated in distributed coupled hydrological models, or even in standalone groundwater models, provides a valuable aquifer parameterization alternative.

INTRODUCTION

In the last decades groundwater became widely used for water supply because of its better quality so lower treatment costs as compared to surface water and because of reduction of water abstraction cost (Llamas and Martínez-Santos 2005). However the prospection and quantification of groundwater is difficult due to subsurface heterogeneity. An improvement in the efficiency of evaluation and management of groundwater resources is needed to mitigate the increasing pressure of the demand, particularly in arid and semi-arid water limited environments.

For quantification of groundwater resources at the catchment scale, distributed numerical hydrological models are considered optimal. However, to provide a valuable management tool, such models need appropriate acquisition of reliable spatial and temporal input data (Lubczynski 2011, Lubczynski and Gurwin 2005). A classic way to gather subsurface parameters to set up hydrological models is through borehole drilling and pumping tests. However, that method is invasive, expensive and time consuming. Non-invasive hydrogeophysical methods allow to complement the invasive methods, in an efficient and economically sound way. The application of such methods as a support for catchment scale, distributed hydrogeological models has recently received significant attention (Frances and Lubczynski 2011, Mahmoudzadeh *et al.* 2012). Dam and Christensen (2003) demonstrated that an improvement of the hydraulic conductivity field is possible using non-invasive techniques but depends on num-

* coprolog@yahoo.com

ber, location and uncertainty of the geophysical observations. The disadvantage of classical non-invasive geophysical techniques is that they often cannot be used as a straightforward support for hydrogeological models. For instance, Andersen *et al*. (2012) showed that relying on transient electromagnetic (TEM) can lead to different interpretations of hydrogeology of buried valleys when different inversion processes are applied. This is the main reason why many researchers, except of exploration purpose, apply classical, non-invasive hydrogeophysics only for qualitative assessment, to interpret the reality with the aim of building conceptual hydrogeological models. For example, an integrated study of Francese *et al*. (2009), combining geological data with three-dimensional resistivity tomography and shallow seismic surveys, was carried out in fractured sandstone aquifer in Tuscany (Italy) to assess the interrelation between tectonics and groundwater circulation. In the northern Matabeleland (Zimbabwe), TEM and continuous vertical electrical sounding (CVES) were used to upgrade the hydrogeological conceptual model: CVES was applied to define the near surface geological structures and TEM to define the deeper structures (Danielsen *et al*. 2007). In Okavango Delta (Botswana), time domain electromagnetic method (TDEM) was used to study three dimensional salinity anomalies (Bauer-Gottwein *et al*. 2010) otherwise difficult to define and interpret. In the Föhr Island (Germany) airborne electromagnetics (SkyTEM) and seismic reflections were compiled into a 3D model (Burschil *et al*. 2012) that was meant as a basis for a groundwater flow model. In Denmark, a strong effort in near-surface geophysical data integration resulted in the development of Sequential Hydrogeophysical Inversion (SHI), in which inverted geophysical models provide information for hydrologic models (Herckenrath 2012).

In contrast to classical geophysical methods, MRS is the only geophysical method that can provide quantitative assessment of water in subsurface. Through assessment of signal amplitude, the MRS is sensitive to the quantity of water in the subsurface and through the signal decay, to permeability of the medium in which the subsurface water is stored and flows. The MRS technique is already known and well accepted as providing a non-invasive, quantitative evaluation of water in subsurface rather than as a prospecting hydrogeophysical tool. More information about principles of the MRS technique with emphasis on quantification of groundwater resources can be found in: Lubczynski and Roy (2003), Lubczynski and Roy (2004), Lubczynski and Roy (2007), Plata and Rubio (2007), Plata and Rubio (2008), Roy and Lubczynski (2003); the parameterization of aquifers in Boucher *et al*. (2009), Lubczynski and Roy (2005), Lubczynski and Roy (2007), Vouillamoz *et al*. (2007), Vouillamoz *et al*. (2012); and parameterization of unsaturated zone in Mohnke and Yaramanci (2008), Roy and Lubczynski (2005), Walsh *et al*. (2012).

The ability of MRS to retrieve subsurface flow and storage parameters of hydrological systems makes it suitable not only for site-specific studies but also for distributed modelling studies, for example focusing at groundwater resources assessment at the catchment scale. To our knowledge, the first such application was documented by Lubczynski and Gurwin (2005) in their groundwater modelling study case of granitic Sardon Catchment in Spain. Later, Lubczynski and Roy (2007) provided a detailed and systematic protocol on how to integrate MRS output in distributed groundwater models. The follow up of practical implementation of such MRS integration was presented by Boucher *et al*. (2009) who later extended that study (Boucher *et al*. 2012) integrating information obtained from 35 MRS soundings in a groundwater model of 5000 km^2 in a sedimentary aquifer in Niger. In that model, previously calibrated using TDEM data but without MRS support, it was possible to narrow down the uncertainty related to water content and hydraulic conductivity of the investigated aquifer by integrating MRS and TDEM inversion results.

In this study, we also propose MRS data integration in a hydrologic model, however in contrast to previous studies we do not consider MRS output as the implicitly known input of a hydrologic model, but instead apply a novel data integration method and optimize MRS-hydrogeological parameters (hydraulic conductivity and specific yield) within the hydrological model calibration. The proposed MRS data integration is carried out by applying the distributed, coupled, hydrologic MARMITES-MODFLOW (MM-MF) model https://code.google.com/p/marmites/ (Francés *et al*. 2011) in the Carrizal Catchment study area in Spain. The catchment is well characterized by availability of time series of water table and soil moisture records but there is a lack of borehole logs and pumping tests. Besides, the position of aquifer bottom is unknown as the Carrizal hydrogeological system is permeable down to more than 100 m, i.e. deeper than the penetration depth of the Numis^{LITE} MRS instrument we used and there are no boreholes penetrating that depth.

Before this study, the Carrizal Catchment had been investigated by MRS technique within a collaboration project (Plata *et al*. 2009) carried out between IGME, University of Madrid and ITC Faculty of University Twente, as documented in Uriarte Blanco *et al*. (2011). In this study, we used the previously acquired MRS data as well as our newly acquired MRS data, and reprocessed all the data using the newest MRS inversion tool Samovar 11.3 (Legchenko 2011).

MATERIAL AND METHODS

Study area

The Carrizal Catchment of 73 km^2 (corner geographic coordinates 41°19'N/5°38'W and 41°12'N/5°27'W), is located in the centre of Duero Basin (Fig. 1). The main Carrizal stream is a left tributary of the Guareña River, tributary of the Duero River. The Carrizal Catchment is characterized by hilly landscape that varies from 745 to 924 m.a.s.l. The climate is dry, Mediterranean, with semi-arid characteristics (Ceballos *et al*. 2002), mean precipitation of 485 mmy^{-1} and FAO 56 Reference Evapotranspiration (Allen *et al*. 1998) of 1093 mmy^{-1}, as measured at Villamor

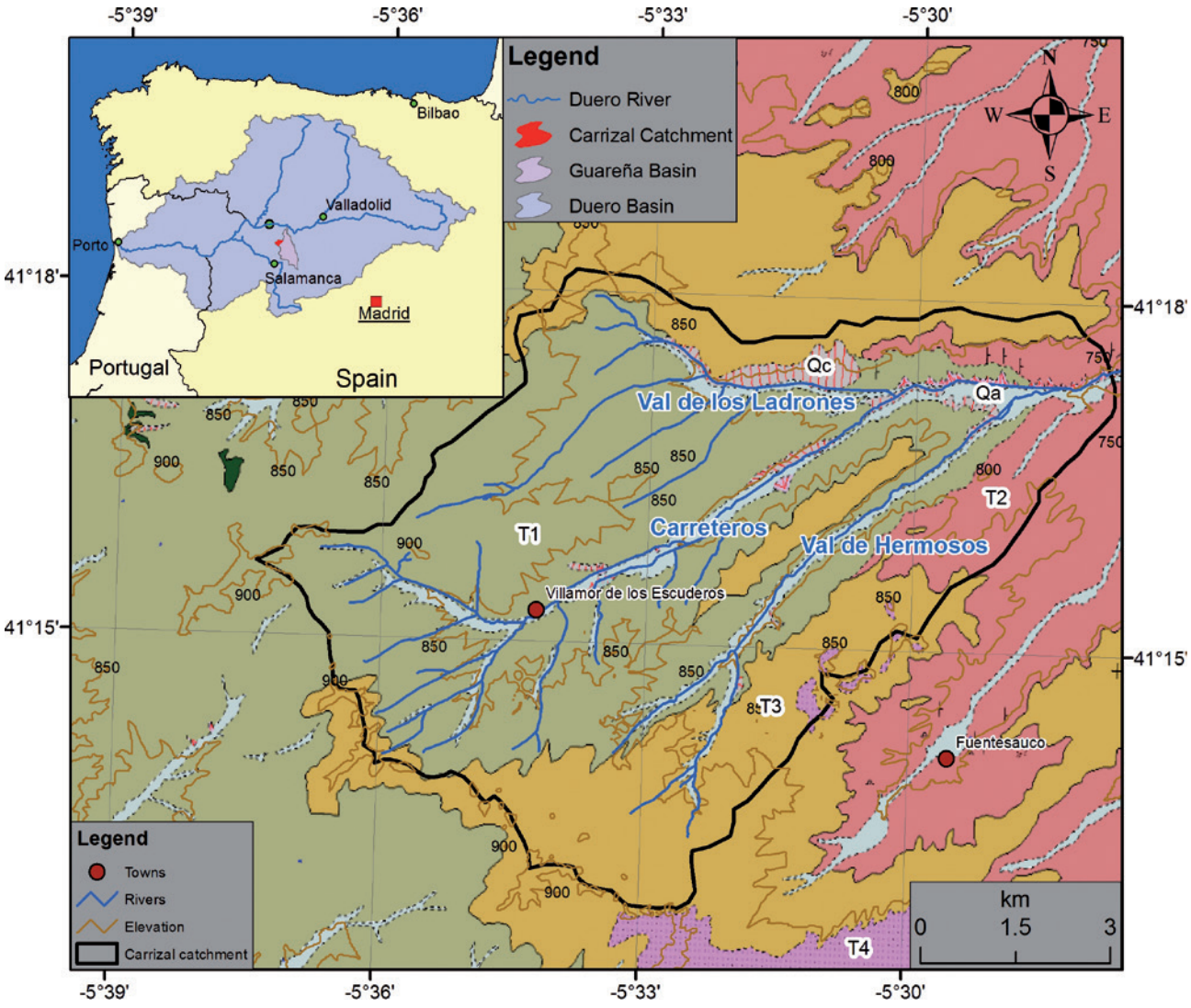

FIGURE 1

Geology of the study area (Instituto Geológico y Minero de España 1978, Instituto Geológico y Minero de España 2000): T_1 – Cabrerizos Sandstones (Middle Eocene – Oligocene), silts and sandstones with conglomeratic levels; T_2 – Low Palaeogene Group (Middle Eocene – Oligocene), thin layers of sandstones, conglomerates and silts; T_3 – High Palaeogene Group (High Eocene – Oligocene), thick layers of sandstones, microconglomerates, siltites and arkoses with cobbles; T_4 – Red Series (High Eocene – Lower Miocene), conglomerate, quartzite and silts; Qc – Coluvium (Pliocene – Holocene), cobbles, boulder sands, silts and clays; Qa – Alluvium (Middle Pleistocene – Holocene), cobbles, pebbles, sands, silts and clays.

weather station. The Carrizal Catchment belongs to the REMEDHUS Soil Moisture Network of Salamanca University (Martínez-Fernández and Ceballos 2005).

The geology of the study area (Fig. 1) is characterised by continental deposits from Palaeogene and Quaternary. The Palaeogene formations are sub-horizontal and constitute detritical, fluvial deposits mainly composed of conglomerates, sandstones and siltstones with carbonate or clay cement. These formations result from the lateral motion of stream channels across floodplain, which explains the high lateral and depth-wise lithofacial variability. The thickness of the Palaeogene formations is around 100 m, although it reaches 500 m at Tarazona de Guareña, located 15 km from the study area in the east direction (Instituto Geológico y Minero de España 1978). The bottom of the valleys in the Carrizal Catchment is covered by thin alluvial deposits and colluvium of Quaternary age composed of sandstones, silts, cobbles and clays that result from erosion and sequential deposition of the Tertiary rocks. These geological settings result in a heterogeneous hydrogeological configuration, particularly in the Tertiary formations. Although some relatively shallow lenticular levels can produce interesting yields and can be explored by boreholes, many drillings (none in the Carrizal Catchment) are negative. Following the hydrogeological map of IGME at the scale 1:200 000 available at www.igme.es/infoigme/visor/, the hydraulic conductivity (K) is

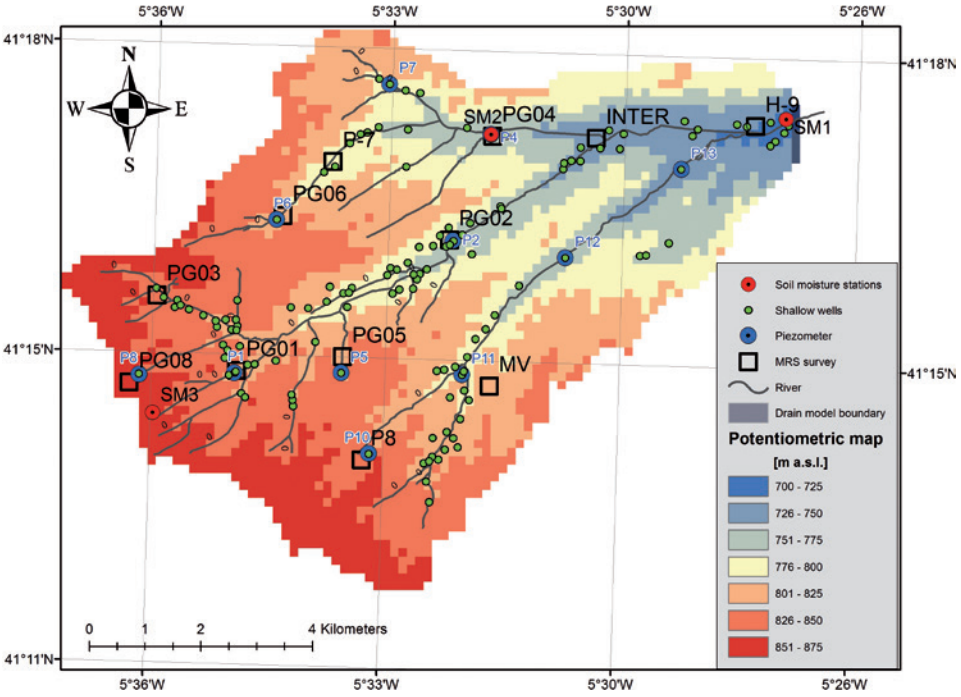

FIGURE 2
Monitoring network of the Carrizal Catchment; at the background groundwater potentiometric map.

intermediate in the Tertiary formations and high in the Quaternary ones. The transmissivity of the Palaeogene is between 10 and 150 m^2day^{-1} with an average of 50 m^2day^{-1} (Instituto Geológico y Minero de España 2000). The Quaternary formation is unconfined and in direct hydraulic connection with a Tertiary formation. Because of its large *K*, the Quaternary aquifer is widely exploited using large diameter wells for agricultural use.

The potentiometric surface of the shallow unconfined aquifer (Fig. 2) was defined based on field measurements of altitude, water table depth and the linear relationship established between topography and hydraulic head following the method described in Kuniansky *et al*. (2009). An intense field campaign was carried out in November 2009 when the hydraulic head was defined in 136 shallow wells by conjunctive measurements of well elevations using a differential GPS (Leica GPS model 1200 using Real Time Kinematics protocol) and water table depths using standard deeper.

As this study is part of a broader, PhD project, focused on groundwater recharge in the shallow unconfined aquifer, significant effort was dedicated not only to saturated but also to unsaturated zone assessment. The soil investigations carried out at 5 cm depth in a regular grid of 3 by 3 km within the REMEDHUS area were spatially densified within the scope of this study in a grid of 1 km^2, to better describe soil texture spatially. These investigations defined quite homogeneous sandy loam soil type, characterized by a typical composition of 66% sand, 18% clay and 16% silt. The depth-wise homogeneity of the soil hydraulic properties and texture was also confirmed at piezometer locations down to a depth of 3 metres. The thickness of the unsaturated zone varied in the study area from some tens of cm in the bottom valley near the Carreteros stream at the center of the Carrizal Catchment, up to more than 10 metres in the Val de los Ladrones valley in the north of the Carrizal Catchment (Fig. 1). Aquifer parameters were not available due to the lack of boreholes to perform pumping tests. The few available, shallow (1–14 m depth), wide dimension wells (2–6 m wide) were not pump tested because it would require heavy logistic (e.g., high performance pump) and financial investments, not available in this study.

The Carrizal study area was equipped with a monitoring network (Fig. 2) that allowed us to retrieve the driving forces (rain and potential evaporation and transpiration) and the state variables (soil moisture and hydraulic heads) necessary to run and calibrate the distributed hydrologic model. The monitoring network involved: i) 3 soil moisture profiles, each with moisture probes installed at 5, 25, 50 and 100 cm depths, all recording hourly since November 2009; ii) an automated microclimatic weather station at the Villamor location (41°14'N–5°36'W), measuring precipitation, air temperature, incoming radiation, wind speed and relative humidity every 10 minutes, with 9 years of data available (2002/2010); and iii) 11 automated groundwater level recorders installed in 11 piezometers, recording hourly since November 2009.

General description of the MM-MF model

Groundwater model solutions are generally affected by non-uniqueness due to the multiplicity of combinations between parameters, such as hydraulic conductivity or storativity, and fluxes, such as groundwater evapotranspiration, exfiltration and recharge. Not only realistic system parameterization but also the introduction of realistic spatio-temporally variable water fluxes

verified in transient model calibration, allow us to restrict non-uniqueness and improve the reliability of models (Lubczynski and Gurwin 2005). In this study, the spatio-temporal variability of water fluxes was simulated by the coupled MARMITES-MODFLOW (MM-MF) model (Francés *et al*. 2011) as the coupled models are known to better handle the calibration non-uniqueness than standalone models such as the MODFLOW alone (Furman 2008).

The MARMITES (MM) is a transient, distributed model of the land surface and the soil zone that is coupled with the groundwater MODFLOW (MF) model. Both models share the same spatial and temporal discretization. Figure 3 shows the structure of one cell of the MM-MF model. MM is composed of one surface component (MARMITESsurf) and one soil zone component (MARMITESsoil). The unsaturated zone below the soil zone bottom and above the water table is modelled using UZF1 package of MODFLOW-NWT (Niswonger *et al.* 2011) and the groundwater flow by MODFLOW itself. The data exchange between MM and MF is shown in Fig. 4. The models are run sequentially until the average difference of groundwater heads computed by the two last sequential runs are less than a predefined threshold, generally 10^{-3} m. The MARMITESsurf (Fig. 3) computes the driving forces of the hydrological cycle, i.e. rainfall, potential evaporation and transpiration using the Penman-Montheith equation as formulated in Allen *et al*. (1998). It requires as input hourly, continuous time series of the following meteorological data: rainfall, wind speed, air relative humidity, air temperature and incoming solar radiation. Vegetation, soil maps and parameters are also required. Next, the water balance in the soil zone of MARMITESsoil is computed on a daily basis using lumped-parameters and linear relationships between fluxes and soil moisture. The soil zone is discretized into superimposed layers that are parameterized with basic soil hydraulic properties (porosity, specific retention, wilting point, saturated hydraulic conductivity and thickness). Generally these soil layers are defined using textural criterion and correspond to the A and B horizons, which are the zones of eluviation and illuviation respectively (Dingman 2002). The user is also free to define one single soil zone that corresponds to the root zone. The intermediate, subsoil layer of unsaturated zone is modelled using the UZF1 (Niswonger *et al*. 2006) package of MF and corresponds to the C and R zones, i.e. parent material and bedrock respectively (Dingman 2002). The UZF1 converts percolation from the soil computed by MARMITESsoil into groundwater recharge applying kinematic-wave approximation of the Richard's equation (Niswonger *et al*. 2006). If the water table reaches the bottom of the soil layer, exfiltration from the aquifer into the soil zone occurs. Finally, water flow and storage in the saturated zone are computed by MF. The transient calibration of the MM-MF coupled models is typically done against soil moisture in MM and hydraulic heads in MF.

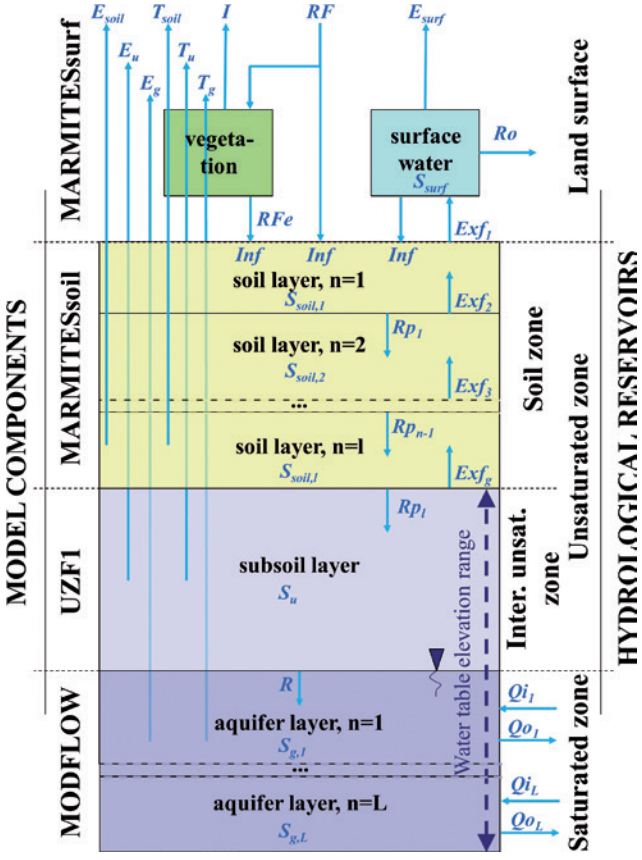

FIGURE 3

Conceptual schema of one vertical cell of the coupled MM-MF model (Francés *et al*. 2011), showing various model components handling water fluxes within the following hydrological reservoirs: 1) Land surface: rainfall (*RF*), rainfall excess (*RFe*), interception (*I*), evaporation from open water (E_{surf}), surface runoff (*Ro*), storage (S_{surf}); 2) Soil: infiltration (*Inf*), evaporation (E_{soil}), transpiration (Ts_{oil}), percolation (*Rp*), exfiltration (*Exf*), storage (S_{soil}); 3) Subsoil: evaporation (E_u), transpiration (T_u), storage (S_u); 4) Saturated zone: evaporation (E_g), transpiration (T_g), recharge (R), exfiltration (Exf_g), inflow/outflow (*Qi/Qo*), storage (S_g).

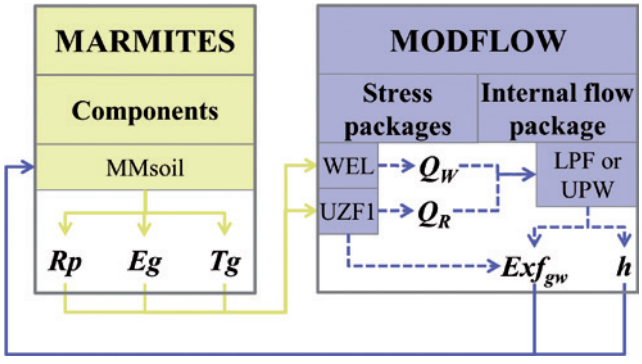

FIGURE 4

Coupling of MARMITES and MODFLOW models (Francés *et al*. 2011); *h* is hydraulic head, for other abbreviations see Fig. 3.

Setup and calibration of the Carrizal MM-MF model

The distributed Carrizal MM-MF hydrological model consisted of 91 columns and 69 rows of quadratic grid, with 3267 active cells, 150x150 m each. The topographic surface was defined by a 5 m high resolution digital elevation model provided by the STIG (Servicio Transfronterizo de Información Geográfica) of Salamanca University resampled to 150x150 m MM-MF model grid. Following the results of the soil survey described earlier, we defined three soil types, one in the top part of the catchment, one in the lower part and one along the main streams (i.e. alluvium). The top boundary of the aquifer was defined as elevation minus the soil thickness. The piezometric surface (Fig. 2) represented by altitude of the shallow water table (hydraulic head) on November 2009, was used as the initial head condition for the model. The lateral boundaries of the model were assigned along the Carrizal Catchment watershed divide that matches groundwater divide, except of the eastern catchment outflow section simulated by MF Drain Package boundary conditions (Fig. 2). As there were no borehole logs available and the regional hydrogeological knowledge suggested the presence of a thick, permeable, sedimentary sequence down to the depth significantly larger even than 100 m b.g.s., based on the analysis of the 12 MRS soundings, we decided to schematize arbitrarily that system into one, unconfined layer of fixed thickness of 35.5 m. That thickness was assigned as equal to the shallowest inversion depth among all the MRS-inverted profiles (Fig. 7), counting from the water table depth defined by direct field measurements. Further reasoning of that assignment can be found below in the Results and Discussion.

The first two years of data were used in the transient model simulation as spinoff (initialization) period, i.e. giving the model time to reach equilibrium under applied forces, while the other three years were used for the calibration process. The soil moisture in the MMsoil module of the MM-MF model was manually calibrated against daily soil moisture measurements in 3 Stevenswater, soil moisture Hydra Probe sensors (www.stevenswater.com), each located at 25 cm depth. That calibration aimed at the definition of spatio-temporally variable net recharge. Two indexes were calculated to analyse the goodness of fit between simulated and observed soil moisture curves: (i) the RSR of Moriasi *et al*. (2007) that is the root mean square error (RMSE) normalized by standard deviation (SD) of the observed heads; and (ii) the Pearson's correlation coefficient (r). While the RSR is a measure of discrepancy between the simulated and observed soil moisture, the r shows how well model and observation trends fit each other. The soil moisture calibration was carried out by adjusting soil field capacity and soil thickness towards laboratory and field defined ranges, focusing on minimizing RSR and maximizing the Pearson's correlation coefficient (r).

The groundwater MODFLOW module of the MM-MF model was calibrated against time series of hydraulic head measurements in 11 piezometers. The water levels in piezometers were recorded by Keller (www.keller-druck.com) automated water table recorders. The head calibration was done by adjustment of multipliers of MRS estimates of specific yield ($S_{y,MRS}$) and MRS estimates of hydraulic conductivity (K_{MRS}). In every calibration run, one multiplier for the 12 $S_{y,MRS}$ and another one for the 12 K_{MRS} were assigned, which guaranteed the original proportionality between the 12 MRS estimates of specific yield and hydraulic conductivity. The MODFLOW calibration of heads was carried out by trial and error adjustment of the two MRS multipliers focusing on minimizing RSR at the 11 monitored piezometers and maximizing the Pearson's correlation coefficient (r). That calibration allowed us, finally, to select a pair of MRS multipliers that could be further used to estimate specific yield (S_y) and hydraulic conductivity (K) at the 12 MRS survey locations as explained below.

MRS contribution to hydrogeological parameterization

Distributed hydrological models, such as MM-MF, require definition of hydrostratigraphic layers, aquifer parameters and water fluxes. The main aim of the MRS measurements in this study was to characterize spatial variability of hydraulic parameters of the shallow unconfined aquifer by integrating the MRS measurements in a coupled hydrological MM-MF model optimizing the MRS estimates of specific yield ($S_{y,MRS}$) and hydraulic conductivity (K_{MRS}).

Hydrogeophysical pre-MRS field measurements

Pre-MRS field measurements were carried out prior to the MRS surveys assessing: i) natural magnetic field (B); ii) electromagnetic noise; and iii) geoelectrical subsurface profiles using Vertical Electrical Sounding (VES) or TDEM. The magnetic field and noise measurements were carried out to confirm suitability of a selected site for the MRS survey and to optimize survey at that site (Lubczynski and Roy 2004), whereas the geoelectrical profiles supported the MRS inversion process. The assessment of natural magnetic field was executed to determine local scale magnetic inhomogeneity and to determine Larmor frequency (f_l) necessary for the MRS survey. The magnetometric survey was carried out with two magnetometers: geometric G856 as rover and a G816 as a base in 12 selected MRS survey sites. In each selected MRS site, 36 magnetometric measurements were carried out within 100x100 m quadratic or rhomboid area. The electromagnetic noise and the VES/TDEM measurements were performed in the pre-selected MRS-survey locations. The noise measurements were done with a coil especially designed for the noise investigation (Plata *et al*. 2009). The VES investigations were executed with a Syscal R2E resistivity meter from IRIS instruments while the TDEM measurements with a 50 m square loop using a TEM-FAST 48 from Applied Electromagnetic Research (AEMR).

MRS field measurements

The selection of the MRS sounding locations was a result of careful GIS-based analysis of the land cover, available subsurface information and pre-MRS field measurements. That selection attempted also to cover hydrological variability within the Carrizal

Catchment and to have shallow wells nearby, to provide direct information on the groundwater table depth as auxiliary data in the MRS water detection process. As a result 12 MRS locations were selected. In each site, the magnetic field (B) was measured directly before the MRS survey and the retrieved value was used to calculate the Larmor frequency required for the MRS survey. Since B varied with time, we also monitored its temporal variations during the MRS survey. The 12 selected MRS locations were surveyed in two field campaigns, the first in April 2009 with 8 soundings (Uriarte Blanco *et al*. 2011) and the second in November 2009 with 4 soundings. In both campaigns, the Numis^{Lite} MRS equipment manufactured by IRIS-Instruments (2012) was used. The locations of the MRS sounding experiments are presented in Fig. 2. The 12 MRS surveys resulted in satisfactory data coverage of 1 MRS survey per ~6 km^2, essential for appropriate constrain of the distributed hydrological model. In the 8 MRS surveys, a 60 m square-shaped loop was used while in the 4 surveys, due to lower signal to noise (S/N) ratios, a square-8 loop of 30 m side each, oriented parallel to adjacent electric power lines, was used with the aim of improving the S/N ratio. That configuration allowed us to work in areas with a relatively low S/N ratio, where the standard 60 m square-shape loop would not permit to perform MRS sounding correctly (Trushkin *et al*. 1994).

MRS data processing

For the inversion of the MRS sounding data, the new Samovar V.11.3 (Legchenko 2011) was used. At each MRS survey location, the geoelectrical profiles acquired through VES and/or TDEM were used in the calculation of the Samovar "linear filter". The linear filter is a pre-calculation of the MRS response at the given location for a suite of theoretical layers at increasing depth levels, taking into account the MRS loop shape and size, the range of excitation moment (Q), the subsurface geoelectrical layering in terms of resistivity and thickness, the Earth's magnetic field magnitude and its inclination.

The transient model of the unconfined Carrizal aquifer required pre-assignment of spatial variability of the specific yield. Following Legchenko (2004), Lubczynski and Roy (2003), Lubczynski and Roy (2005), Lubczynski and Roy (2007), Vouillamoz *et al*. (2012), in medium to coarse grain materials such as the composition of the shallow Carrizal aquifer, the following MRS assumption is valid:

$$\Theta_{MRS} \approx n \tag{1}$$

where: Θ_{MRS} – MRS free water content obtained as a result of MRS survey and n – porosity;
From standard hydrogeology (Fetter 2001):

$$n = S_y + S_r \tag{2}$$

where: S_y – specific yield and S_r – specific retention also known as field capacity.

Therefore combining equations 1 and 2 we obtain:

$$\Theta_{MRS} \approx S_y + S_r \tag{3}$$

In equation 3, the unknown S_r prevents direct estimate of S_y from equation 3. The equation 3 indicates also that $S_y \leq \Theta_{MRS}$, where the difference between the two increases towards finer material of the aquifer, i.e. larger S_r. This observation is also reflected in empirical equation 4 in Vouillamoz *et al*. (2012) that presents linear relation of MRS estimate of specific yield ($S_{y,MRS}$) with Θ_{MRS} as follows:

$$S_{y,MRS} = 0.4*\Theta_{MRS} + 0.0056 \tag{4}$$

According to Vouillamoz *et al*. (2012), the equation 4 is valid for sandy deposits if $0.7 < \Theta_{MRS} < 5.4\%$. Boucher *et al*. (2009) suggested that for such low values of Θ_{MRS}, the linearity of the equation is fairly well maintained but for larger Θ_{MRS} the relationship is not always perfectly linear. Because the Carrizal study area is relatively small and hydraulically uniform, it can be assumed that the variability of the specific yield is well resembled by the 12 MRS surveys available. Therefore the 12 $S_{y,MRS}$ values were calibrated (by trial and error) by optimizing the storage multiplier (m) in equation 5:

$$S_y = mS_{y,MRS} \tag{5}$$

where m – storage multiplier, the same for all MRS measurements.

Initially, the 12 $S_{y,MRS}$ values were estimated according to the equation 4. These values were spatially interpolated using inverse distance weighted method with power 1 (IDW1), this way creating preliminary MM-MF model input matrix. The IDW1 method was selected based on Robinson and Metternicht (2006) and Kravchenko and Bullock (1999), because of the low skewness distribution of our data suggesting low exponent. Next the multiplier m was introduced as proposed in the equation 5 and further optimized by trial and error in the MM-MF transient model calibration to find optimal m specific for the Carrizal aquifer, that best facilitates the agreement between the simulated and measured heads, i.e. with the lowest RSR and highest r.

Another parameter that is required by the MM-MF model is hydraulic conductivity (K). To obtain it, first, for each of the 12 MRS-surveys, the MRS estimates of aquifer transmissivity (T_{MRS}) were derived according to equation 6 applying Samovar 11.3 inversion with its default $C_{T0} = 7*10^{-9}$

$$T_{MRS} = C_{T0} * \Sigma\Theta_{MRS}(z) * (T_1)^2\Delta z \tag{6}$$

where C_{T0} - Samovar 11.3 default MRS-transmissivity multiplier; $\Theta_{MRS}(z)$ - MRS free water content at depth z; T_1 - longitudinal relaxation time in milliseconds; Δz thickness of individual layer in meters.

In the next step, each transmissivity value was converted to hydraulic conductivity according to equation 7:

$$K_{MRS} = \frac{T_{MRS}}{z_{tot}} \quad (7)$$

where K_{MRS} – hydraulic conductivity derived by MRS; $z_{tot} = \Sigma\Delta z$ – total thickness of the aquifer in metres. The final aquifer transmissivity and hydraulic conductivity are expressed by equations 8 and 9 respectively.

$$T = C_T * \Sigma\Theta_{MRS}(z) * (T_1)^2\Delta z \quad (8)$$

$$K = \frac{T}{z_{tot}} \quad (9)$$

After defining 12 T_{MRS} values according to the equation 6, i.e. applying $C_{T0} = 7*10^{-9}$, the 12 K_{MRS} were calculated according to equation 7 and further interpolated using the IDW1 method creating a preliminary K_{MRS} MM-MF model input matrix. Next, the multiplier C_T was introduced as in equation 8 and 9 and further optimized in the MM-MF transient model calibration in order to find optimal C_T value that best facilitates the agreement between the simulated and measured heads (lowest RSR and highest *r*).

RESULTS AND DISCUSSION

An overview of the environmental conditions of the 12 MRS surveys characterizing their suitability for MRS soundings is presented in Table 1. The magnetic inhomogeneity (ΔB) varied among the MRS-sites from 2 to 12 nT (Table 1). Two of the 12 sites are presented in Fig. 5 as examples of the Carrizal Catchment magnetic field variability within the MRS loop scale. It can be observed that at the site INTER, with 60x60 m square loop (Fig. 5a), the magnetic field was fairly constant (ΔB = 6 nT), while at the PG05 with square-8 loop (Fig. 5b), variability of the magnetic field was larger (ΔB = 10 nT). In general the magnetic inhomogeneity within the MRS survey sites of the Carrizal Catchment was low as the largest ΔB in H-9 location (Table 1) did not exceed 12 nT, i.e. Δf_l = 0.5Hz on the Larmor frequency which can be considered as nearly homogeneous field condition. The pre-MRS noise survey indicated low electromagnetic noise ranging from 375 to 650 nV (Table 1) suitable for MRS surveys in 11 out of the 12 selected locations. The only one location where the noise was too high was discarded and replaced with a new, nearby location, H-9, with lower, compared to other sites, noise. At PG02, PG05, PG08 and P-8, due to the presence of adjacent electric power lines, a square-8 loop configuration parallel to the power line had to be used to reduce the noise influence. During the MRS experiments the environmental noise did not vary much, typically staying within 200 nV difference (Table 1); however, in the two sites, i.e. PG04 and P-7, the MRS measurements had to be repeated because of temporally variable noise.

The VES and TDEM results inverted into resistivity layers were used as support of the MRS inversions. In order to characterize variability of the resistivity attributed to the modelled, shallow aquifer extent, for each MRS survey location, the aquifer resistivity (Table 2) at each surveyed site was estimated by the weighted average of the resistivity layers within the aquifer thicknesses as defined by the MRS soundings. Except for the M-V location with relatively large resistivity of 190 Ωm, in all other locations the resistivities were low, in the order of 10–30 Ωm. The results of the 12 MRS surveys, inverted with Samovar 11.3 using preliminary standard $C_{T0} = 7*10^{-9}$ and corresponding geoelectrical profiles, are presented in Table 2 and

TABLE 1

Description of the MRS surveys: L – loop shape and size; B_{avg} – magnetic field averaged in each MRS survey location; ΔB – range of magnetic field inside the loop in each MRS survey location (magnetic inhomogeneity).

	UTM_X	UTM_Y	Survey date	L	Stacking	B_{avg}	ΔB	Noise
units	[m]	[m]	dd/mm/yy	[m]	No	[nT]	[nT]	[nV]
PG01	283669	4569517	4/21/2009	SQ-60	64	44877	9	450-650
PG02	287486	4571856	4/27/2009	SQ8-30	120	44875	9	550-650
PG03	282246	4570870	4/30/2009	SQ-60	96	44882	4	400-550
PG04	288259	4573714	4/23/2009	SQ-60	96	44905	7	500-600
PG05	285569	4569759	11/4/2009	SQ8-30	120	44908	10	445-465
PG06	284502	4572292	11/3/2009	SQ-60	100	44897	6	380-540
P-7	285402	4573260	4/21/2009	SQ-60	96	44889	7	375-475
P-8	285900	4567914	11/3/2009	SQ8-30	96	44871	3	410-490
PG08	281744	4569307	11/3/2009	SQ8-30	100	44877	7	300-400
H-9	292973	4573888	4/28/2009	SQ-60	96	44895	12	450-550
M-V	288197	4569233	4/28/2009	SQ-60	96	44875	2	400-550
INTER	290121	4573677	11/4/2009	SQ-60	120	44915	6	410-510

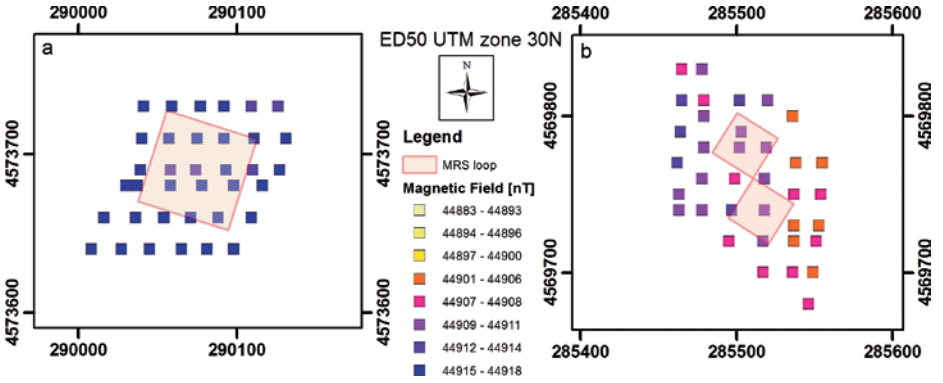

FIGURE 5
Magnetic field in MRS experiments: a) MRS-loop location with medium magnetic field variability (INTER); b) MRS-loop location with higher magnetic field variability (PG05).

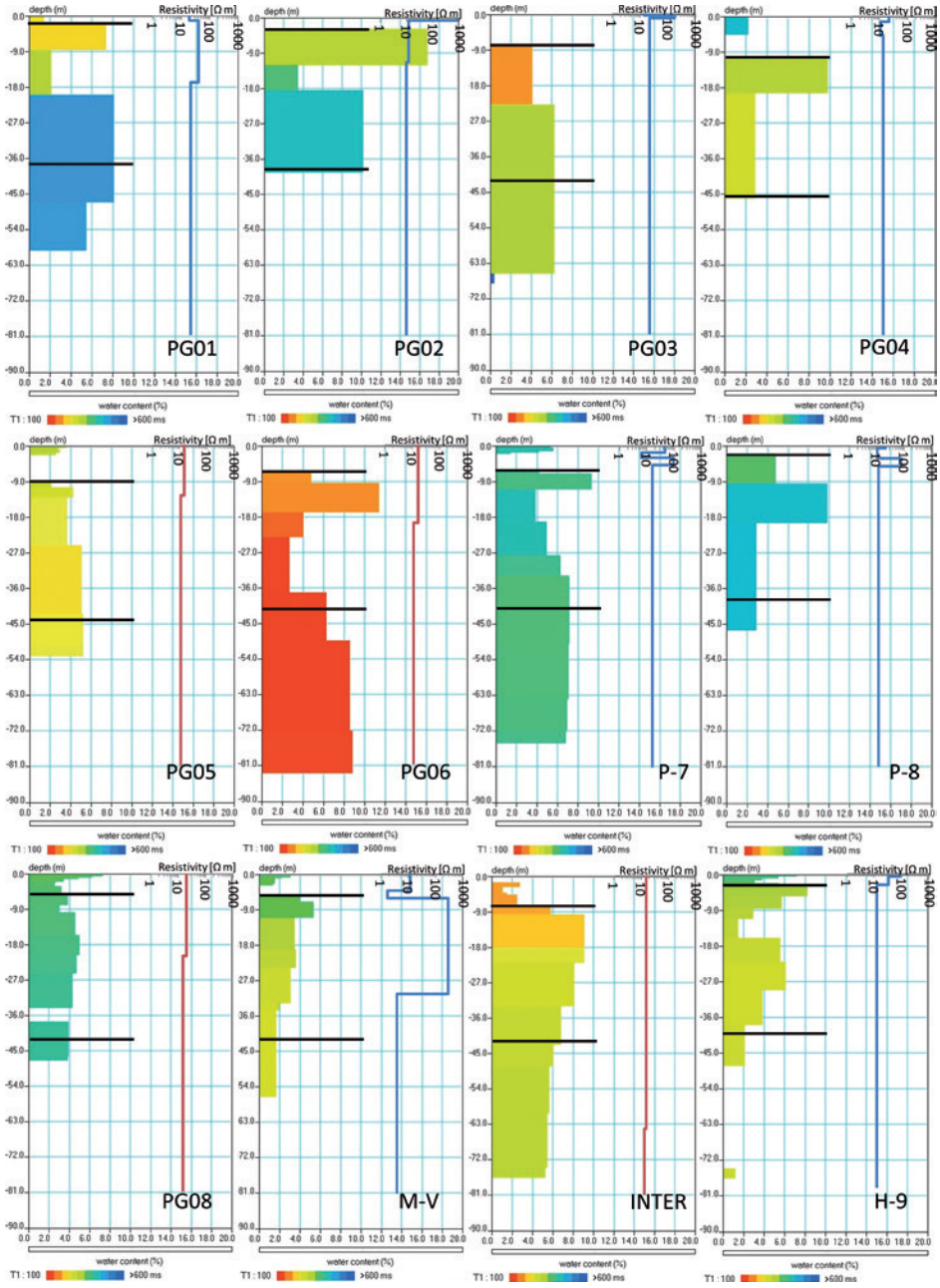

FIGURE 6
Scaled MRS inversion results of Θ_{MRS} and T_1 with preliminary, standard, $C_{T0} = 7*10^{-9}$. Black lines show the assigned in the hydrologic model top and bottom aquifer boundaries. On the right side of each image, resistivity profiles in logarithmic scale are shown by blue line for VES and brown line for TDEM method.

TABLE 2

MRS survey results: *GWTD* – ground water table depth; *D* – thickness of the aquifer; ρ – resistivity of the aquifer; Θ_{MRS} – MRS water content of the aquifer; T_1 – decay time constant; $S_{y,MRS}$ – MRS estimator of specific yield; K_{MRS}, T_{MRS} – MRS estimators of hydraulic conductivity and aquifer transmissivity based on standard multiplier $C_{T0} = 7*10^{-9}$; S_y – calibrated specific yield; K – calibrated hydraulic conductivity using optimized MRS-transmissivity multiplier C_T .

MRS	Altitude	*GWTD*	*D*	ρ	Θ_{MRS}	T_1	$S_{y,MRS}$	T_{MRS}	K_{MRS}	S_y	K
units	[m.a.s.l.]	[m]	[m]	[Ω m]	%	[ms]	%	[m^2 d^{-1}]	[m d^{-1}]	%	[m d^{-1}]
PG01	850	1.9	>57	30	6.1	390	2.4	246	6.9	2.4	3.4
PG02	792	2.8	>37	10	10.8	400	4.3	357	10.1	4.3	5.0
PG03	872	7.7	>58	22	5.3	262	2.2	95	2.7	2.2	1.3
PG04	777	10.5	35.5	13	4.6	274	1.8	83	2.3	1.8	1.1
PG05	846	9.1	>44	11	4.4	229	1.8	49	1.4	1.8	0.7
PG06	825	6.5	>76.5	13	5.5	124	2.2	23	0.6	2.2	0.3
P-7	810	6.2	>69	16	5.9	415	2.4	213	6.0	2.4	3.0
P-8	853	2.0	>44	15	5.2	440	2.1	218	6.2	2.1	3.1
PG08	877	5.4	>42	17	3.9	409	1.6	134	3.8	1.6	1.6
M-V	835	4.0	>53	190	3.2	296	1.3	65	1.8	1.3	0.9
INTER	763	6.5	>70.5	15	7.9	245	3.2	102	2.9	3.2	1.4
H-9	751	3.0	45	15	4.7	302	1.9	84	2.4	1.9	1.2
Mean		6.3		31	5.6	315	2.3	137	3.4	2.3	1.9
St.Dev		2.8		31	2.0	96	0.8	96.6	2.8	0.8	1.4

Fig. 6 whereas the location of the 12 MRS surveys can be found in Fig. 2. In order to enhance readability of the MRS survey results, all the MRS profiles were presented within the same depth range, water content and decay time scales. Due to the excitation limit of the NUMIS^{Lite} equipment and the loop size up to L = 60 m, the Samovar inversions of the MRS surveys allowed for the maximum investigation depth < 90 m b.g.s., which for the four surveys with square-8 loop (PG02, 437 PG05, PG08 and P-8) was still significantly lower.

All the MRS surveys were realized next to shallow wells or piezometers with known groundwater table depth (*GWTD*) of < 6 m b.g.s. In all survey locations, the MRS detected *GWTD* with an acceptable error of some tens of centimetres. For example *GWTD* at PG01 was 1.9 m while the corresponding depth manually measured in the nearby well was 2.2 m. Such high MRS accuracy in *GWTD* detection was expected as the MRS survey conditions were favourable (Table 1) and also because MRS detectability at shallow depth is typically very good.

In the MODFLOW model, we assigned an unconfined layer with spatially uniform thickness 35.5 m delimited by two black lines in Fig. 6, upper representing phreatic water table and lower arbitrarily assigned aquifer bottom, based on the shallowest (counting from the water table) penetration depth of the MRS-inverted sounding profiles. Such schematization was made because: 1) in the Carrizal Catchment there is no impermeable layer within the depth range of the MRS investigation that could be assigned as bottom boundary of the model; 2) spatially uniform thickness guaranteed that the estimated transmissivity is not influenced by uncertain MRS estimates of aquifer depth; 3) the assigned thickness had to have the largest possible depth to cover the largest possible spectrum of groundwater flow; 4) the model aquifer top, i.e. the water table, was defined with high confidence and confirmed by direct measurements in nearby wells; 5) the model aquifer bottom was restricted by availability of experimental data, i.e. the lack of sufficiently deep boreholes and by MRS penetration depth in PG04 and PG02 (Fig. 6); 6) the groundwater flow in aquifers, such as in the unconfined Carrizal aquifer, is typically shallow and laterally dominant, as horizontal hydraulic conductivity is typically an order of magnitude larger than vertical (Fetter 2001); therefore the shallow lateral streamlines contribute the most to the overall groundwater flow of the catchment.

The applied uniform aquifer thickness schematization, discards some valuable information provided by MRS at the deepest parts of some MRS sounding profiles but offers the following advantages: i) assures that the optimized transmissivity is only hydraulic conductivity dependent so not biased by subjective selection of aquifer bottom; ii) creates the possibility of applying the method we propose in this paper, requiring that the proportions between the 12 MRS estimates are valid; iii) captures the most MRS-trustable and hydrogeologically-important for the model performance, shallow section of the aquifer.

The proposed schematization of the Carrizal model has important implications. The assignment of only one layer

implies a 2D groundwater model solution with only lateral component of flow. Besides, in MODFLOW, the bottom boundary of the lowest aquifer is automatically assigned impermeable. In reality, the Carrizal aquifer extends deeper than the assigned bottom boundary of our model. This implies that the calibrated net recharge applied to the aquifer compensates the eventual bottom boundary flux that would occur if there was no arbitrary no-flow bottom boundary at depth of 35.5 m from the water table; nevertheless it is expected that the bottom flux in the Carrizal Catchment is low or even negligible as the shallow aquifer has quite large horizontal hydraulic conductivity in the order of 10 md^{-1}, favouring shallow-lateral flow with a short residence time (Fetter 2001).

The MMsoil model calibration of soil moisture provided a good match between measured and simulated soil moisture, and as a result generated spatio-temporally variable net recharge that was further used as input in MODFLOW calibration. An example of soil moisture calibration for the selected time series SM1 sensor measurements is presented in Fig. 7. That calibration shows good agreement between simulated and measured soil moisture records and was characterized with r = 0.87 and RSR = 0.51. The head calibration in MODFLOW was completed after 49 runs, each time with different values of m and C_T, although not all the runs were stable. The unstable runs are marked in white in the two left panels in Fig. 7. The best, optimized model solution based on three years of head calibration with the lowest RSR = 4.28 and the highest r = 0.74, was obtained for m = 1 and $C_T = 3.5*10^{-9}$. The $S_{y,MRS}$ is best defined using r while the K_{MRS} using RSR. This is because $S_{y,MRS}$ variations influence the amplitude of the piezometric curve, thus the trend and the fitting between simulated and observed curves to which r is sensitive, while K_{MRS} variations modify the distance (offset) between the two curves, which is reflected in the RSR value. An example of modelled and observed head in one piezometer P1 with a well-retrieved pattern of temporal variability of water table fluctuation is shown in Fig. 7. The shift between modelled and observed heads is a consequence of model scale: the Carrizal model is set up with a resolution of 150x150 m, so the P1 head observation has likely incurred a shift due to the topographically constrained head variability within the grid cell. Nevertheless, the most important in transient model calibration temporal pattern of head measurements (Lubczynski and Gurwin 2005) was well retrieved.

The $S_{y,MRS}$ input parameter of the MM-MF model estimated using equation 4 (Vouillamoz *et al*. 2012) is listed in Table 2. We used equation 4 to estimate $S_{y,MRS}$ even though our average Θ_{MRS} was 5.6%, i.e. slightly above the range recommended by Vouillamoz. The estimated $S_{y,MRS}$ varied from 1.3% in PG04 to 4.3% in PG02, with a mean of 2.3% and standard deviation σ = 0.8%. It is remarkable that through the model calibration, the m multiplier was not changed (m = 1) so that $S_{y,MRS}$ did not need any adjustment in the process of transient model calibration, implying $S_{y,MRS} \sim S_y$ according to equation 5. The difference between S_y and $S_{y,MRS}$ was within the resolution of calibration process, which shows that the MRS estimate of specific yield ($S_{y,MRS}$) using equation 4 provided a good guess of S_y in the Carrizal Catchment.

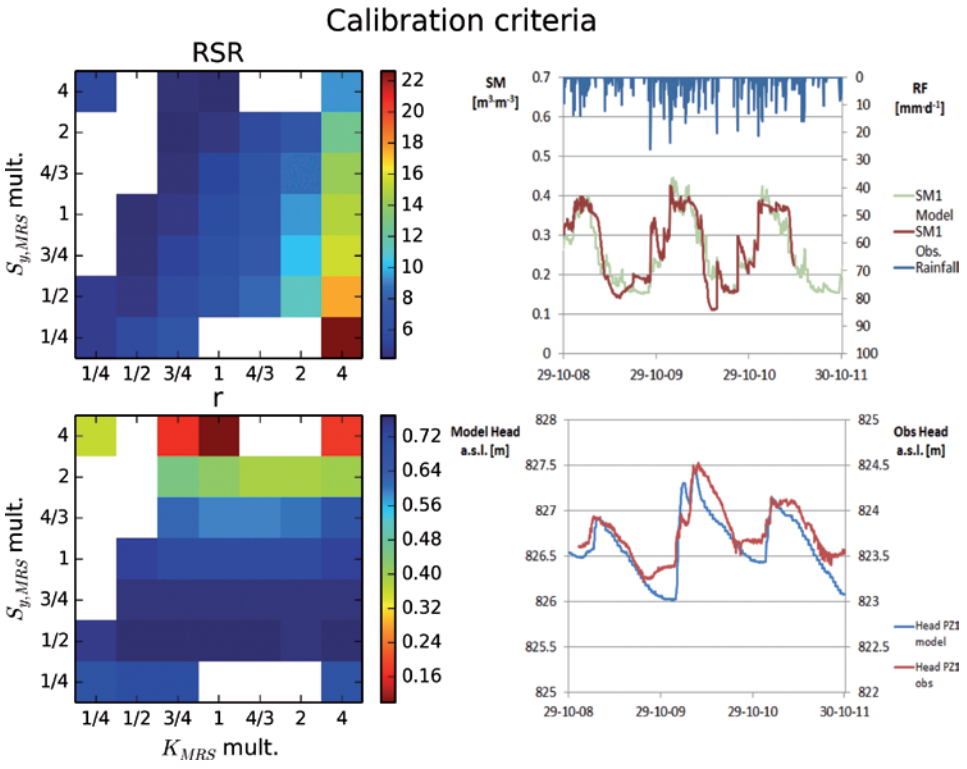

FIGURE 7
Calibration analysis. The two panels at the left show RSR (upper panel) and r (lower panel) computed in relation to simulated and observed hydraulic heads and varying the multipliers of MRS estimators of specific yield ($S_{y,MRS}$) and hydraulic conductivity (K_{MRS}); in white combination of parameters that do not provide a stable solution in MM-MF model, in dark blue best solution. The two panels at the right present examples of model calibration of soil moisture at SM1 location (upper part) and hydraulic head at PG1 (lower part).

Figure 8 shows spatial distribution of S_y in the Carrizal Catchment that ranged from 1% to 4.5%, pointing at significant aquifer homogeneity.

The K_{MRS} input parameter of the MM-MF model estimated using equations 6 and 7, is listed in Table 2. The K_{MRS} varied from 0.6 md^{-1} in PG06 to 10.1 md^{-1} in PG02 with a mean of 3.9 md^{-1} and standard deviation σ = 2.8 md^{-1}. The optimized in the calibration of groundwater model C_T = 3.5*10^{-9} is specific for the Carrizal Catchment. Considering that initially used in the calibration C_{T0} = 7*10^{-9}, the optimized in MM-MF K was only twice lower than K_{MRS} (Table 2). The optimized K varied from 0.3 md^{-1} in PG06 to 5.0 md^{-1} in PG02 with a mean of 1.9 md^{-1} and standard deviation σ = 1.4 md^{-1}. Considering that hydraulic conductivity is spatially log-normally distributed (Fetter 2001), the spatial variability of the Carrizal Catchment K presented in Fig. 9, can be considered as very low pointing at significant aquifer homogeneity.

Despite low spatial variability of S_y and K, there was still some internal variability in the estimates of $S_{y,MRS}$ and K_{MRS}, although not large. For example, relatively large differences within $S_{y,MRS}$ and K_{MRS} were observed between PG02 and PG05 locations (Table 2). We analysed granulometry of the soil samples from 3 m depth in these two locations to see if what was depicted by MRS Θ_{MRS} and T_1 did indeed properly reflect field lithological and hydrogeological differences. We found that the soil material in the PG02 contained 79% of sand and was coarser than in the PG05 that contained 56% of sand. This was in line with the MRS $S_{y,MRS}$ and K_{MRS} estimates and confirmed that MRS was well able to depict the hydrogeological differences between different survey locations despite these differences being quite low.

The comparison of our optimized C_T = 3.5*10^{-9} with Uriarte Blanco *et al*. (2011) of the same Carrizal Catchment is not straightforward as they applied different Samovar version 6.2 for the inversion while we used Samovar version 11.3. The two inversions led to different results because of different software characteristics and different investigated thicknesses. Nevertheless, their C_T value was quite similar to ours, varying from 0.18*10^{-9} to 25.4*10^{-9}. Even more similar were C_T values derived in clayey-sands in France (4.9*10^{-9}) by Vouillamoz (2003) and in sands in Niger (17*10^{-9}) by Vouillamoz *et al*. (2007).

When comparing our study with the similar study integrating MRS in the distributed groundwater model presented by Boucher *et al*. (2012), we had larger spatial density of the MRS surveys, investigated a much smaller area and used a different method of MRS data integration in groundwater model. Instead of facilitating groundwater model with data provided by MRS, we used transient groundwater model to optimize MRS multipliers, m and C_T, which allowed us to optimize S_y and K based on $S_{y,MRS}$ and K_{MRS} respectively. In our Carrizal case, the S_y and K did not change much as compared to corresponding $S_{y,MRS}$ and K_{MRS}, which confirmed the appropriate performance of MRS in the hydrogeological conditions of Carrizal Catchment. However, in other more heterogeneous areas the same methodology can also be applied. The proposed methodology of aquifer parameterization based on optimizing m and C_T multipliers in distributed hydrological models, represents an alternative to the method of cross referencing MRS surveys with pumping test data. Like the other method that uses pumping test data implicitly, our method also offers an opportunity of defining m and C_T multipliers which

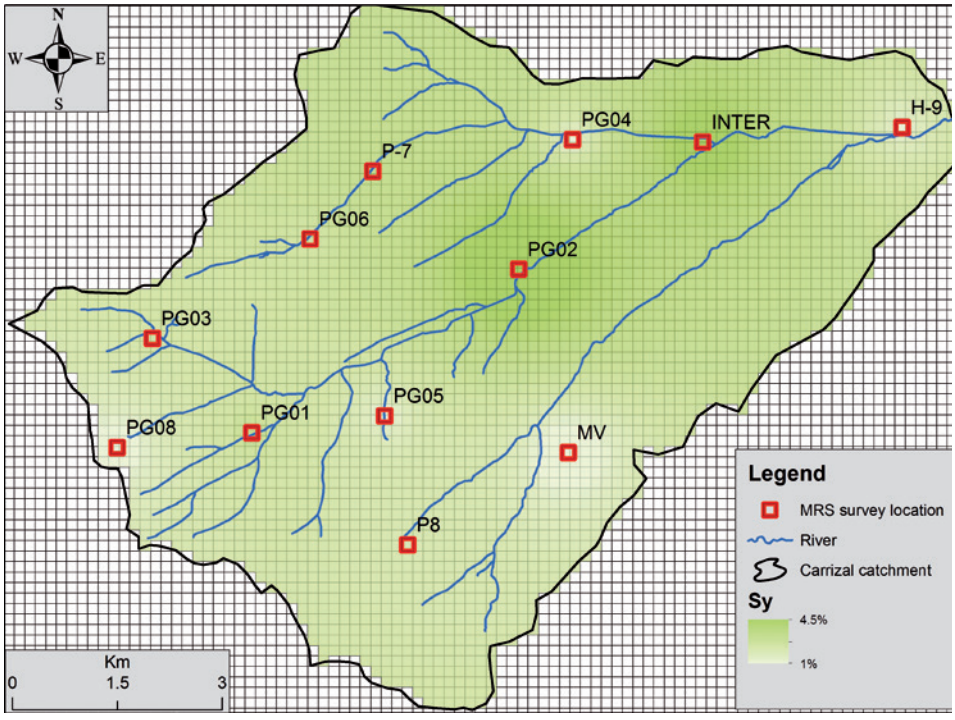

FIGURE 8
Distribution of the calibrated specific yield (S_y).

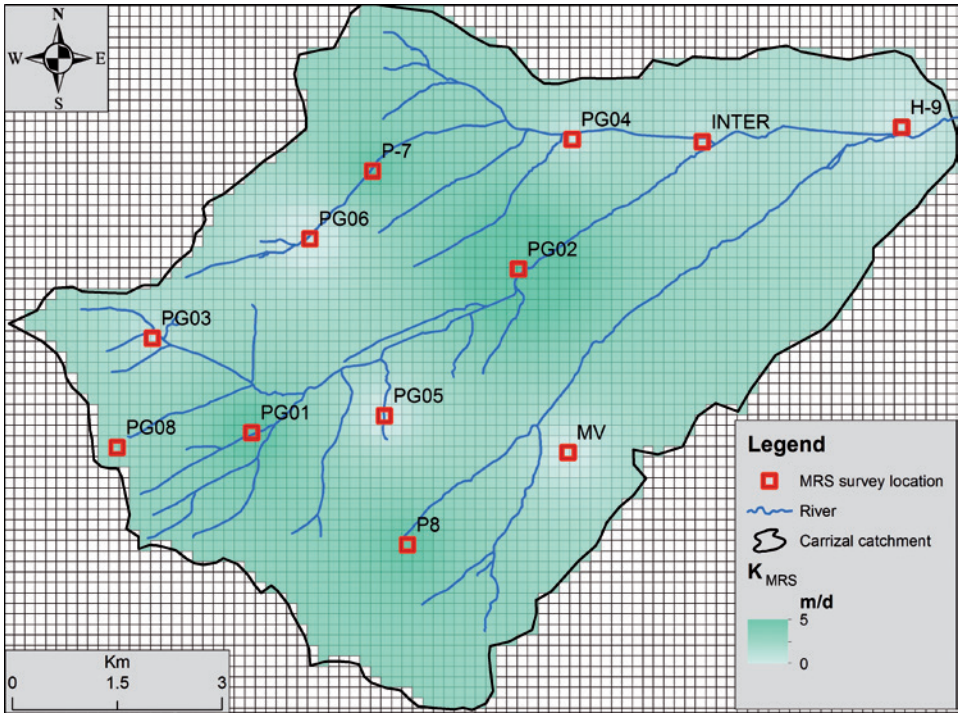

FIGURE 9
Distribution of the calibrated hydraulic conductivity (K).

are characteristic for the investigated area. This means, that in the case of follow up MRS surveys in that area (or adjacent, hydrologically similar areas), these multipliers can be used for direct estimates of aquifer S_y, T and K. The proposed method does not need pumping test data, but requires a good quality modelling input data (preferably long time series data) allowing for a tight constrain of a calibrated, distributed and preferably coupled, transient hydrological model, although a solution applying a standard, standalone groundwater model would also suffice.

When calibrating a steady-state model, only a C_T multiplier can be derived. Both, m and C_T multipliers can be derived in transient models. The most effective hydrological model constrain and therefore the highest reliability can be achieved in transient and coupled models such as the presented Carrizal model – in transient, because calibration against temporal data optimally reduces hydrological model non-uniqueness (Lubczynski 2011), and in coupled, because such models handle the aquifer input fluxes in a more reliable manner than standalone models (Francés *et al*. 2011, Furman 2008). If in an investigated area, pumping tests are available, then certainly they should be used as model input, because they enhance reliability of models. However, if not available, then the proposed optimization method is an opportunity that should be considered if appropriate data to set up a model is available. The important question related to the applied optimization method, but also to the common practice of calibrating MRS results with pumping test data is, when and under which conditions in an investigated area, only one storage (m) and only one transmissivity multiplier (C_T) representative for that investigated area can be applied. We hypothesize that m and C_T depend on hydraulic model of groundwater flow at the pore scale of analysed aquifers. In that respect there are 4 main types of such hydraulic models: primary porosity (e.g., unconsolidated sand), secondary porosity (e.g., fractured granite); double porosity (e.g., sandstone) and karst (e.g., limestone). If in an investigated study area, there are rocks of different hydraulic models, then certainly different m and different C_T have to be introduced. However, whether within investigated rock types of the same hydraulic model but differing for example by texture or lithology, only one m and one C_T can be used, this requires further testing and cross-referencing with pumping tests that unfortunately were not available in this study.

CONCLUSIONS

The MRS technique is highly suitable for its integration with distributed, hydrological models because: i) it provides quantitative estimates of storage and flow parameters (S_y, T, K) at the survey location; ii) the volumes investigated by MRS survey can be easily adjusted in a distributed hydrological model by grid and layering adjustment so that the two are comparable in scale.

We proposed a novel method of integrating MRS results in a distributed, coupled transient hydrological model using Carrizal Catchment study area as an example. In this method we assumed that individual MRS sounding results can be biased but the relative differences between MRS survey results at different locations of the catchment reflect real hydrological differences between these locations. Following that assumption, we assigned specific yield and transmissivity multipliers (m and C_T respectively) to the corresponding MRS-specific yield and MRS transmissivity estimators and optimized the two multipliers in the transient, coupled hydrological model calibration.

The MRS integration with hydrological model of the Carrizal Catchment area allowed us to: i) calibrate the model; ii) derive $m = 1.0$ and $C_T = 3.5*10^{-9}$ that can be used in future MRS investigations in the Carrizal Catchment (and/or adjacent areas with similar hydrogeological conditions) to convert MRS survey results into hydrogeological output; iii) acquire spatial variability of specific yield and transmissivity/hydraulic conductivity in the Carrizal Catchment; the obtained parameters showed pretty low spatial variability, pointing at significant aquifer homogeneity; iv) present and explain the proposed, novel method of MRS data integration in hydrological model.

The values of MRS estimators of specific yield and transmissivity/hydraulic conductivity defined in the Carrizal Catchment were close to the corresponding, finally optimized values of specific yield (S_y) and hydraulic conductivities (K); this confirmed the functional capability of MRS in quantitative aquifer parameterization.

If pumping tests are available, then they should be used to define MRS multipliers of the hydrogeological parameters; however if not available, but there is enough data to set up a coupled, distributed hydrological model or at least a standalone groundwater model, then the MRS integration method proposed in this study provides a valuable alternative that should be further tested in various hydrogeological conditions against pumping test data.

ACKNOWLEDGMENTS

We would like to acknowledge Fundación Instituto Euromediterráneo del Agua and ITC for the financial support in the field campaign investigation, the IGME and ETSIM of Madrid and especially Clara Uriarte, Juan Luis Plata, Jesus Diaz Curiel and Lucia Arevalo Lomas for the collaboration in the field and IRD in person of Anatoly Legchenko for the NUMIS^{Lite} loan. José Francisco Charfole, Marta Rodrìguez Ruiz and Ana Cano Crespo for the help in the GPS pre-MRS field campaign and Pilar Alonso Rojo for the help in the laboratory analysis.

REFERENCES

Allen R.G., Pereira L.S., Raes D. and Smith M. 1998. *Crop Evapotranspiration: Guidelines for Computing Crop Water Requirements*. FAO, Rome.

Andersen T.R., Poulsen S.E., Christensen S. and Jørgensen F. 2012. A synthetic study of geophysics-based modelling of groundwater flow in catchments with a buried valley. *Hydrogeology Journal* **20**. doi:10.1007/s10040-012-0924-5

Bauer-Gottwein P., Gondwe B.N., Christiansen L., Herckenrath D., Kgotlhang L. and Zimmermann S. 2010. Hydrogeophysical exploration of three-dimensional salinity anomalies with the time-domain electromagnetic method (tdem). *Journal of Hydrology* **380**, 318–329.

Boucher M., Favreau G., Descloitres M., Vouillamoz J.M., Massuel S., Nazoumou Y. *et al*. 2009. Contribution of geophysical surveys to groundwater modelling of a porous aquifer in semiarid Ntiger: An overview. *Comptes Rendus Geoscience* **341**, 800–809. doi:10.1016/j.crte.2009.07.008

Boucher M., Favreau G., Descloitres M., Vouillamoz J.M., Massuel S., Nazoumou Y. *et al*. 2009. Contribution of geophysical surveys to groundwater modelling of a porous aquifer in semiarid niger: An overview. *Comptes Rendus – Geoscience* **341**, 800–809.

Boucher M., Favreau G., Nazoumou Y., Cappelaere B., Massuel S. and Legchenko A. 2012. Constraining groundwater modeling with magnetic resonance soundings. *Ground Water* **50**, 775–784. doi:10.1111/j.1745-6584.2011.00891.x.

Boucher M., Favreau G., Vouillamoz J.M., Nazoumou Y. and Legchenko A. 2009. Estimating specific yield and transmissivity with magnetic resonance sounding in an unconfined sandstone aquifer (Niger). *Hydrogeology Journal* **17**, 1805–1815. doi:10.1007/s10040-009-0447-x

Burschil T., Scheer W., Kirsch R. and Wiederhold H. 2012. Compiling geophysical and geological information into a 3-d model of the glacially-affected island of Föhr. *Hydrology and Earth System Sciences* **16**, 3485–3498. doi:10.5194/hess-16-3485-2012

Ceballos A., Martínez-Fernández J., Santos F. and Alonso P. 2002. Soil-water behaviour of sandy soils under semi-arid conditions in the Duero Basin (Spain). *Journal of Arid Environments* **51**, 501–519.

Dam D. and Christensen S. 2003. Including geophysical data in groundwater model inverse calibration. *Ground Water* **41**, 178–189.

Danielsen J., Dahlin T., Owen R., Mangeya P. and Auken E. 2007. Geophysical and hydrogeologic investigation of groundwater in the karoo stratigraphic sequence at sawmills in Northern Matabeleland, zimbabwe: A case history. *Hydrogeology Journal* **15**, 945–960.

Dingman S.L. 2002. *Physical Hydrology*. Prentice Hall, Upper Saddle River.

Fetter C.W. 2001. *Applied Hydrogeology*. Merril Publishing, Upper Saddle River, NJ.

Francés A.P. and Lubczynski M.W. (2011) Topsoil thickness prediction at the catchment scale by integration of invasive sampling, surface geophysics, remote sensing and statistical modeling. *Journal of Hydrology* **405**(1–2), 31–47.

Francés A.P., Reyes-Acosta J.L., Balugani E., van der Tol C. and Lubczynski M.W. 2011. Towards an improved assessment of the water balance at the catchment scale: A coupled model approach. In: Estudios en la zona no saturada del suelo: volumen X : ZNS11 proceedings, 19–21 October 2011, Salamanca, Spain: e-book / editor J.M. Fernández, , N.S. Martin. Salamanca: Universidad de Salamanca, 2011. 370 p. ISBN 978-84-694-6642-1. pp. 321-326.

Francese R., Mazzarini F., Bistacchi A., Morelli G., Pasquarè G., Praticelli N. *et al*. 2009. A structural and geophysical approach to the study of fractured aquifers in the Scansano-Magliano in Toscana Ridge, Southern Tuscany, Italy. *Hydrogeology Journal* **17**, 1233–1246.

Furman A. 2008. Modeling coupled surface-subsurface flow processes: A review. *Vadose Zone Journal* **7**, 741–756. doi:10.2136/vzj2007.0065

Herckenrath D. 2012. Informing groundwater models with near-surface geophysical data. Ph.D Thesis, TechnicalUniversity of Denmark.

Instituto Geológico y Minero de España. 1978. Mapa geológico de España. Hoja 426 (Fuentesauco). In: *Mapa geológico de España*.

Instituto Geológico y Minero de España. 2000. Mapa geológico de España. Hoja 425 (Villamor de los Escuderos). In: *Mapa geológico de España*.

IRIS-Instruments. 2012. www.Iris-instruments.Com.

Kravchenko A. and Bullock D.G. 1999. A comparative study of interpolation methods for mapping soil properties. *Journal of Agronomy* **91**, 393–400.

Kuniansky E.L., Lowery M.A. and Campbell B.G. 2009. How processing digital elevation models can affect simulated water budgets. *Ground Water* **47**, 97-107.

Legchenko A. 2011. Samovar software 11.3 User's Guide.

Legchenko A., Baltassat, J.-M., Bobachev, A., Martin, C., Robain, H. and Vouillamoz, J.-M. 2004. Magnetic resonance sounding applied to aquifer characterization. *Ground Water* **42**, 363–373. doi:10.1111/j.1745-6584.2004.tb02684.x

Llamas M. and Martínez-Santos P. 2005. Intensive groundwater use: Silent revolution and potential source of social conflicts. Editorial. *Journal of Water Resources Planning and Management* **131**, 337–341.

Lubczynski M. and Roy J. 2003. Hydrogeological interpretation and potential of the new magnetic resonance sounding (MRS) method. *Journal of Hydrology* **283**, 19–40.

Lubczynski M. and Roy J. 2004. Magnetic resonance sounding: New method for ground water assessment. *Ground Water* **42**, 291–303. doi:10.1111/j.1745-6584.2004.tb02675.x

Lubczynski M.W. 2011. Groundwater evapotranspiration - underestimated role of tree transpiration and bare soil evaporation in groundwater balances of dry lands. In: *Groundwater evapotranspiration – underestimated role of tree transpiration and bare soil evaporation in groundwater balances of dry lands*, (eds A. Baba, G. Tayfur, O. Gunduz, K.W.F. Howard, M.J. Friedel and A. Chambel), pp. 183–190. Springer.

Lubczynski M.W. and Gurwin J. 2005. Integration of various data sources for transient groundwater modeling with spatio-temporally variable fluxes - Sardon study case, Spain. *Journal of Hydrology* **306**, 71–96.

Lubczynski M.W. and Roy J. 2005. MRS contribution to hydrogeological system parameterization. *Near Surface Geophysics* **3**, 131–139.

Lubczynski M.W. and Roy J. 2007. Use of MRS for hydrogeological system parameterization and modeling. *Boletin Geologico y Minero* **118**, 509–530.

Mahmoudzadeh M.R., Francés A.P., Lubczynski M.W. and Lambot S. (2012) Using ground penetrating radar to investigate the water table depth in weathered granites: Sardon case study, Spain. *Journal of Applied Geophysics* **79**, 17–26.

Martínez-Fernández J. and Ceballos A. 2005. Mean soil moisture estimation using temporal stability analysis. *Journal of Hydrology* **312**, 28–38. doi:10.1016/j.jhydrol.2005.02.007

Mohnke O. and Yaramanci U. 2008. Pore size distributions and hydraulic conductivities of rocks derived from magnetic resonance sounding relaxation data using multi-exponential decay time inversion. *Journal of Applied Geophysics* **66**, 73–81.

Moriasi D.N., Arnold J.G., Van Liew M.W., Bingner R.L., Harmel R.D. and Veith L.V.T. 2007. Model evaluation guidelines for systematic quantification of accuracy in watershed simulations. *Transactions of the ASABE* **50**, 885–900.

Niswonger R.G., Panday S. and Ibaraki M. 2011. MODFLOW-NWT, a newton formulation for MODFLOW-2005. In: *MODFLOW-NWT, a Newton formulation for MODFLOW-2005*, pp. 44. U.S. Geological Survey

Niswonger R.G., Prudic D.E. and Regan R.S. 2006. Documentation of the unsaturated-zone flow (UZF1) package for modeling unsaturated flow between the land surface and the water table with MODFLOW-2005. In: *Documentation of the unsaturated-zone flow (UZF1) package for modeling unsaturated flow between the land surface and the water table with MODFLOW-2005*, *Vol. 6*. USGS.

Plata J.L. and Rubio F.M. 2007. Basic theory of the magnetic resonance sounding method. *Boletin Geologico y Minero* **118**, 441–458.

Plata J.L. and Rubio F.M. 2008. The use of MRS in the determination of hydraulic transmissivity: The case of alluvial aquifers. *Journal of Applied Geophysics* **66**, 128–139. doi:10.1016/j.jappgeo.2008.04.001

Plata J.L., Uriarte C. and Martínez-Fernandez J. 2009. Use of MRS to obtain hydraulic parameters and to setup a groundwater model: application in the Arenales shallow aquifer (in Spanish). Uso de los srm para la obtención de parámetros hidráulicos y su implementación en la modelización de aguas subterráneas: Aplicación en el acuífero superficial de los arenales. Informe nº 63790. Centro de Documentación del IGME, 119.

Robinson T.P. and Metternicht G. 2006. Testing the performance of spatial interpolation techniques for mapping soil properties. *Computers and Electronics in Agriculture* **50**, 97–108.

Roy J. and Lubczynski M. 2003. The magnetic resonance sounding technique and its use for groundwater investigations. *Hydrogeology Journal* **11**, 455–465. doi:10.1007/s10040-003-0254-8.

Roy J. and Lubczynski M.W. 2005. MRS multi – exponential decay analysis: Aquifer pore - size distribution and vadose zone characterization. *Near Surface Geophysics* **3**, 287–298.

Trushkin D.V., Shushakov O.A. and Legchenko A.V. 1994. The potential of a noise-reducing antenna for surface NMR groundwater surveys in the earth's magnetic field. *Geophysical Prospecting* **42**, 855–862.

Uriarte Blanco C., Plata Torres J.L., Díaz-Curiel J. and Martínez Fernández J. 2011. The use of magnetic resonance sounding in shallow aquifers in the Duero River Basin (in Spanish). *Aplicación de sondeos de resonancia magnética en acuíferos superficiales de la Cuenca del Duero Boletin geologico y minero* **122**, 345–362.

Vouillamoz J.M. 2003. Characterization of aquifers by a non-invasive technique: the magnetic resonance sounding. These de l'Universite de Paris XI, Orsay, 315. (in French) *La caractérisation des aquifères par une méthode noninvasive: Les sondages par résonance magnétique protonique*.

Vouillamoz J.M., Baltassat J.M., Girard J.F., Plata J. and Legchenko A. 2007. Hydrogeological experience in the use of MRS. *Boletin Geologico y Minero* **118**, 531–550.

Vouillamoz J.M., Chatenoux B., Mathieu F., Baltassat J.M. and Legchenko A. 2007. Efficiency of joint use of MRS and ves to characterize coastal aquifer in Myanmar. *Journal of Applied Geophysics* **61**, 142–154. doi:10.1016/j.jappgeo.2006.06.003

Vouillamoz J.M., Sokheng S., Bruyere O., Caron D. and Arnout L. 2012. Towards a better estimate of storage properties of aquifer with magnetic resonance sounding. *Journal of Hydrology* **458–459**, 51–58. doi:10.1016/j.jhydrol.2012.06.044

Walsh D., Grunewald E., Zhang H., Ferre P. and Hinnell A. 2012. Recent advancements in NMR for characterizing the vadose zone. In: *Recent advancements in NMR for characterizing the vadose zone*. 5th International Workshop on Magnetic Resonance in the Subsurface, September 25 - 27, 2012, Hannover, Germany.